PHYSICAL REVIEW C VOLUME 20, NUMBER 1 JULY 1979

Excitation of $E1$ and $M2$ resonances via (π^-,γ) reactions on $^{16,18}O$

G. Strassner* and P. Truöl
Physik-Institut der Universität Zürich, CH-8001 Zürich, Switzerland

J. C. Alder, B. Gabioud, C. Joseph, J. F. Loude, N. Morel, A. Perrenoud, J. P. Perroud, M. T. Tran, and E. Winkelmann†
Institut de Physique Nucléaire, Université de Lausanne, CH-1015 Lausanne, Switzerland

W. Dahme, H. Panke, and D. Renker
Sektion Physik, Universität München, D-8046 Garching, Germany

H. A. Medicus
Physics Department, Rensselaer Polytechnic Institute, Troy, New York 12181
(Received 11 December 1978)

The photon spectra from the reaction $^{16}O(\pi^-,\gamma)^{16}N$ and $^{18}O(\pi^-,\gamma)^{18}N$ were measured with a high-resolution pair spectrometer. Transitions to 2^- states having $T = 1$ in ^{16}N and $T = 2$ in ^{18}N appear to dominate. Excitation of 1^- states in the giant dipole resonance region, which are the analogs of the levels excited in photoabsorption and inelastic electron scattering on ^{16}O and ^{18}O, respectively, were also observed. The total and partial branching ratios for bound states and giant-resonance transitions are compared with shell-model predictions. Higher admixtures to the predominantly 1p-1h wave functions are found to be necessary to obtain agreement with the measured branching ratios. A new treatment of the continuum and resonance excitation, based on calculations of Ohtsubo *et al.*, is compared with the data.

[NUCLEAR REACTIONS Radiative pion capture; measured photon spectra for $^{16}O(\pi^-,\gamma)^{16}N$ and $^{18}O(\pi^-,\gamma)^{18}N$; deduced transitions and transition strength with $J^\pi = 1^-$, 2^- and $T = 1$ and $T = 2$ respectively; comparison with shell-model calculations.]

I. INTRODUCTION

Besides the traditional reactions of photoabsorption, radiative nucleon capture, and inelastic electron scattering, radiative pion capture has recently become a useful tool for the investigation of the giant-dipole resonance (GDR). As for all electromagnetic processes the transition operator for the pion process is well understood, and since it contains the nucleon spin and isospin, it is particularly well suited for the investigation of the spin-isospin component of the GDR.

The double magic nucleus ^{16}O has been the subject of detailed experimental[1] and theoretical[2] studies. The photon spectrum measured by the Berkeley group for ^{16}O (Ref. 1) confirmed only the 2^- state at $E_x(^{16}N) = 0$ MeV. The GDR excitations were left in a very ambiguous state. Since then more elaborate shell-model calculations performed in the impulse approximation with 1p-1h excitation with and without more complex particle-hole admixtures[3-5] have become available and predict strong 2^- excitations. We therefore decided to remeasure ^{16}O with a rather improved energy resolution and statistics. We, furthermore, investigated the heavier isotope ^{18}O. Both isotopes ^{16}O and ^{18}O are the only even-A isotopic pair measured in (π^-,γ) reactions. It is of interest to compare the two nuclei. In first order one expects nearly identical spectra, since (π^-,γ) couples only to protons. The two extra neutrons outside the ^{16}O core couple to $J = 0$ [predominantly $(d\,\frac{5}{2})^2$] and therefore should play a secondary role in proton-hole neutron-particle excitations. The expected effect of the two neutrons is to modify slightly the absolute branching ratio R_γ due to a "blocking" of neutron orbits and to shift slightly the energy of the p-h excitation due to a "polarization" of the ^{16}O core. Also, since little is known about the spectrum of ^{18}N states, the present study was expected to provide information on the position of 1^- and 2^- states in the $A = 18$ system.

II. EXPERIMENTAL METHOD

The experiments were carried out with the high intensity pion beam $\pi E1$ at the Swiss Institute for Nuclear Research (SIN). Pions with a momentum of 200 or 220 MeV/c were degraded in energy and stopped in targets of $D_2{}^{16}O$ (99%), $D_2{}^{18}O$ (97%), and

$H_2{}^{16}O$ enclosed in plastic containers. The effective target thickness (excluding containers) was 1.15 g/cm^2 with the target placed at 45° to the beam direction. The photons emitted perpendicular to the beam were detected in a 180°-bend pair spectrometer. This high-resolution instrument consisted of a window-frame magnet with a usable field volume of $2.50\times 0.65\times 0.52$ m^3 and a maximum field of 1.1 T. The photons were converted in a 88 μm thick gold foil into electron-positron pairs, which were detected by three multiwire proportional chambers (MWPC). A detailed description of the system is available elsewhere.[6]

The absolute acceptance, its variation with energy, and the line shape were measured with a liquid hydrogen target.[6] For typical conditions of the experiments with $D_2{}^{16}O$ and $D_2{}^{18}O$ an absolute acceptance of $(2.63\pm 0.10)\times 10^{-5}$ with a resolution of 0.9 MeV full width at half maximum (FWHM) for 129.4 MeV photons from the reaction $\pi^- p\to n\gamma$ was achieved. In the experiment with the $H_2{}^{16}O$ target the absolute acceptance was increased to $(4.44\pm 0.29)\times 10^{-5}$, and the resolution for 129.4 MeV photons was 1.2 MeV. The raw data had to be corrected for experimental background contributions originating from the target itself ($\pi^- d\to nn\gamma$, $\pi^- p\to n\gamma$, $\pi^- p\to \pi^0 n$ followed by $\pi^0\to 2\gamma$) as well as from the container, the beam telescope, and the degrading material. This problem was overcome by measuring deuterium, hydrogen, and the empty containers in separate runs. The contribution of the degrader and the beam telescope could be removed by reconstructing the direction of the incoming photons from the observed trajectories of the electron-positron pairs that originated in the converter. By applying cuts on the intersection of the photon direction with a vertical plane containing the beam axis, the nontarget associated photons could easily be discarded. The remaining target associated background was subtracted using the measured high-statistics spectra of deuterium,[7] hydrogen,[6] and the container.

For the $H_2{}^{16}O$ measurements the converter thickness was doubled by using two gold foils with an additional thin multiwire proportional chamber sandwiched in between. This small chamber makes it possible to distinguish the contribution of each converter foil as only the electron-positron pairs from the first converter traverse the chamber and the second gold converter. The additional energy loss in the second converter shifts the photon spectrum from the first converter by 800 keV. After correcting for the average energy loss the contributions of both converter foils can be summed yielding a resolution of 1.2 MeV. The response function was again deduced from the hydrogen calibration measurements. The spectra presented here contain the data with 0.9 MeV resolution as well as with 1.2 MeV resolution, so that the final response function had to be determined from appropriately weighted hydrogen spectra. This yielded a final resolution of 1.1 MeV for ^{16}O and a resolution of 0.9 MeV for ^{18}O. This resolution, which is considerably better than the one of 2 MeV (FWHM) obtained in the previous experiment,[1] allows a more precise energy determination of the excited states and resonances and also permits a separation of several groups of states.

III. EXPERIMENTAL RESULTS

A. General considerations

The photon spectra for both oxygen isotopes displayed in Fig. 1 are quite similar. Strong transitions are observed in the bound-state region at $E_\gamma = 128.0$ MeV for $^{16}O(\pi^-,\gamma)^{16}N$ and at $E_\gamma = 124.5$ MeV for $^{18}O(\pi^-,\gamma)^{18}N$ and in the giant-dipole-resonance region at $E_\gamma \approx 120.0$ MeV for ^{16}O and at $E_\gamma \approx 117.6$ MeV for ^{18}O. The latter resonances are superimposed on a quasi-free continuum due to the $(\pi^-,n\gamma)$ reaction. In the reaction with ^{16}O several additional resonances are clearly observed.

The determination of the energies and partial branching ratios for bound states is fully independent of the way the continuum is described. Even for the states in the giant-resonance region the determination of the peak positions is essentially not influenced by the nonresonant contribution. This information from the experimental data can therefore be compared directly with other reactions and theory. The extraction of partial branching ratios for the states in the unbound region, however, depends on the model used for subtraction of the quasi-free continuum. If theoretical cal-

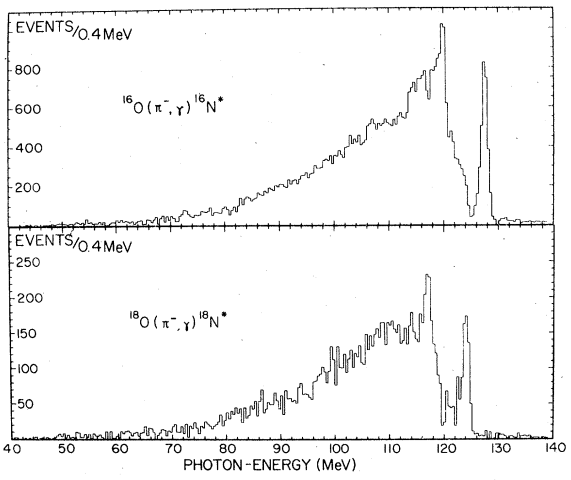

FIG. 1. The photon spectrum for the reactions $^{16}O(\pi^-,\gamma)^{16}N$ and $^{18}O(\pi^-,\gamma)^{18}N$.

culations include continuum transitions as well, such a subtraction is not necessary. However, since most of the available calculations which can be compared with the experimental results do not explicitly treat the continuum, one can in those cases only attempt a comparison by adopting a subtraction procedure. Since interference between the various channels is hereby neglected, this procedure necessarily can only yield results with large uncertainties, which are increased even further by the rather naive models used in the past and also in this paper for the nonresonant contribution. Two different models for the nonresonant contribution have been used.

In the Fermi-gas model one assumes the fundamental radiative interaction of a pion with a proton in the nucleus, whose energy distribution is that of a Fermi gas. No final-state interaction is assumed. In the early low-resolution work by Davies[8] *et al.* with an NaI crystal, the Fermi-gas model was shown to provide a reasonable description of the observed photon spectra.

The pole model suggested by Dakhno and Prokoshkin[9] assumes the exchange of a single proton. The q value at the nucleus vertex is treated as a free parameter, so that the average excitation energy of the nucleus is determined experimentally. It is used here in a slightly modified form (see below).

B. ^{16}O

1. *Transition energies*

The experimental spectrum is well reproduced by a minimum of one line for the unresolved bound-state quartet, three additional lines, and five Breit-Wigner forms superimposed on a nonresonant background for unbound states. Their positions are given in Table I and Fig. 2 together with corresponding energies in ^{16}N and ^{16}O. They were determined by a fit to the data after multiplying with the acceptance and folding in the resolution (Fig. 3). Three different background parametrizations were assumed; the first representing a linear rise from the (^{15}N+n) threshold on, the second following phase space, the third given by a pole model, and finally, no background at all was assumed. In the second and third cases the background was normalized to the data in a region where no resonance excitation is expected. The determined peak positions of the unbound states are independent of the background parametrization used, agreeing within 200 keV. The precision of our energy scale, obtained from the known energy of the hydrogen line, is 50 keV, which reflects the uncertainty of the peak positions for the bound states. The excitation energies of the corresponding levels in ^{16}O were calculated from the excitation energies in ^{16}N assuming a constant Coulomb energy difference deduced from the very well measured state at $E_x(^{16}\mathrm{O}) = 12.9686 \pm 0.0006$ MeV (Ref. 12) of $J^\pi = 2^-$, $T = 1$ in ^{16}O, which is the analog of the ^{16}N ground state.

In Table I the experimental results are given and compared with resonances excited in other electromagnetic processes such as (γ, n) (Ref. 10–13), (γ, p) (Ref. 10, 14, 15), and inelastic electron scattering[16] or (p, γ_0) (Ref. 17) reactions. The photonuclear reactions on ^{16}O excite predominantly states with $J^\pi = 1^-$, $T = 1$, which are also seen in forward inelastic electron scattering.[16] In the latter reaction at higher momentum transfer and backward angles four additional states are clearly identified as $J^\pi = 2^-$, $T = 1$. There is even the indication of a fifth state at an excitation energy of $E_x(^{16}\mathrm{O}) = 23.5$ MeV. The comparison of these excitations with those seen in our experiment offers the possibility of assigning $J^\pi = 1^-$, $T = 1$ to the resonances seen at $E_x(^{16}\mathrm{O}) = 17.1$, 22.12, 24.0, and 25.2 MeV, and $J^\pi = 2^-$, $T = 1$ to those at $E_x(^{16}\mathrm{O}) = 17.7$, 19.1, and 20.4 MeV. The level at 26.4 MeV may be assigned to $J^\pi = 1^-$ of $J^\pi = 2^-$. The 2^- assignment for the dominant structure at $E_x(^{16}\mathrm{O}) = 20.4$ MeV is further supported by the $(p, \gamma_{3\text{-}, 6.13})$ reaction.[18] The level at 20.9 MeV with a $J^\pi = 1^-$, $T = 1$ assignment from (e, e'), (γ, n), and (γ, p) does not appear to be excited strongly in our experiment.

It is somewhat surprising that considerable strength in our experiment is appearing at energies coinciding with $J^\pi = 1^-$, $T = 1$ states observed in photoabsorption, since shell-model calculations as discussed later indicate that for closed-shell nuclei the $J^\pi = 1^-$ isospin and spin-isospin modes of the giant resonance are clearly distinct and well separated in energy by a few MeV. The isospin mode, excited by photoabsorption, is dominated by "non-spin-flip" excitations, while the spin-isospin mode is dominated by the "spin-flip" components. For this mode states are available with $J^\pi = 2^-$ and $J^\pi = 0^-$, which are excluded in the isospin mode. The spin-isospin mode can have spin-flip as well as non-spin-flip components.

2. *Branching ratios*

The partial branching ratio for the bound-state quartet, the dipole resonances, and the continuum nonresonant background are given in Table II. They are determined from the number of events for a given contribution to the final spectrum after background subtraction and corrections for the energy dependence of the acceptance and the loss of photons due to conversion in the target and the anticounters in front of the spectrometer. The

TABLE I. Experimental parameters for radiative pion capture $^{16}O(\pi^-,\gamma)^{16}N$. Comparison of deduced excitation energies with levels seen in other reactions and assigned spins. [$T=1$; all energies in MeV.]

	$^{16}O(\pi^-,\gamma)^{16}N$		$^{16}O(e,e')^{16}O^*$ [a]		$^{16}O(\gamma,n)^{15}N$ [b]		$^{16}O(\gamma,p)^{15}N$ [c]		$^{15}N(p,\gamma_0)^{16}O$ [d]		$^{15}N(p,\gamma_{3^-,6.13})^{16}O^*$ [e]	
E_γ	$E_x(^{16}N)$	$E_x(^{16}O)$	$E_x(^{16}O)$	J^π	$E_x(^{16}O)$	J^π	$E_x(^{16}O)$	J^π	$E_x(^{16}O)$	J^π	$E_x(^{16}O)$	J^π
128.0	0	12.98	12.98	2^-								
123.9	4.1±0.2	17.1±0.2	17.14	1^-	17.3	1^-	17.3	1^-	17.13 17.28	1^- 1^-		
123.2	4.8±0.2	17.7±0.2	17.60	2^-								
121.7	6.1±0.2	19.0±0.2	19.04 19.50	2^- 1^-	19.3	1^-	19.0 19.5	1^- 1^-	19.02 19.52	1^- 1^-	18.98	≥2, 3, 4
120.5	7.5±0.2	20.4±0.2	20.36	2^-	20.9	1^-	20.85	1^-	20.945	1^-	20.40	2^-
118.8	9.1±0.2	22.2±0.2	22.30	1^-	22.2	1^-	22.16	1^-	22.146	1^-		
116.9	11.1±0.2	24.0±0.2	24.20	1^-	24.05	1^-	24.04	1^-	24.065	1^-		
115.8	12.2±0.2	25.2±0.2			25.20	1^-	25.0 25.5	1^- 1^-	25.117	1^-		
114.5	13.5±0.2	26.4±0.2					26.3	1^-				

[a] Reference 16.
[b] Reference 10–13.
[c] References 10, 14, 15.
[d] Reference 17.
[e] Reference 18.

corresponding number of pions stopping in the target is determined from a range curve at low pion beam intensity. The reliability of this procedure was confirmed by our hydrogen calibration experiment.[6] The branching ratio for the sum of the 2^- ground state and the $0^-, 3^-, 1^-$ states 120, 296, and 397 keV above the ground state was found to be $(14.5\pm1.6)\times10^{-4}$. Our instrumental resolution was not sufficient to obtain the four contributions separately. Limiting the fit to the 2^- and the 3^- state, which from theory are expected to be dominant (see Sec. IV 2 b), yielded almost equal contributions for both levels ($2^-/3^- \simeq 1.0\pm0.3$).

For the determination of the resonance contribution the following procedure was adopted. The pole model was used and the residual nucleus after emission of a neutron was assumed to be either in its ground state ^{15}N, $J^\pi = \frac{1}{2}^-, E_x = 0$ or in

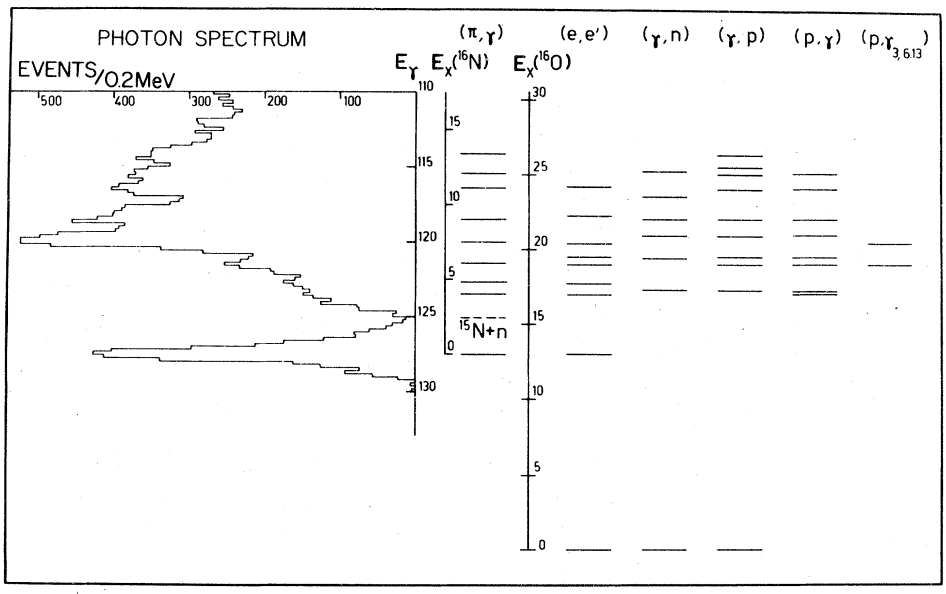

FIG. 2. The photon spectrum for the reaction $^{16}O(\pi^-,\gamma)^{16}N$ in the bound-state and the giant-dipole excitation region. Comparison of observed transitions with levels seen in ^{16}N and ^{16}O.

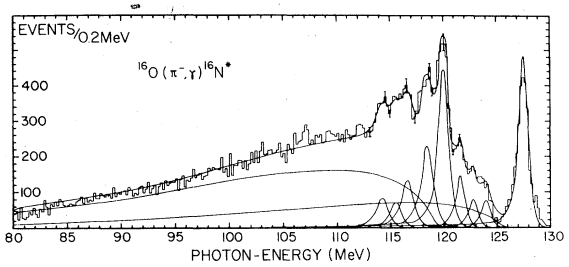

FIG. 3. Photon spectrum of π^- capture in ^{16}O. Solid curve is derived by folding the contributions of the pole models, five Breit-Wigner resonances and four lines with the response function of the apparatus.

its lowest lying excited state of negative parity $^{15}N^*, J^\pi = \frac{3}{2}^-, E_x = 6.3$ MeV. The continuum was then described by the superposition of the two respective pole contributions, neglecting any correlation of both reaction channels. The positive parity states are neglected because the theory predicts a negligible contribution, since such states cannot be excited via a one-body operator.[4,5] Further justification for these parametrizations is found in the continuum shell-model calculations of Ohtsuka and Ohtsubo[19] described in Sec. IV.

The total quasi-free contribution is thus found from the experiment to be $(167 \pm 18) \times 10^{-4}$. Its determination is mainly based on the energy region between 50 and 100 MeV, where no sharp resonances are expected. Below 50 MeV the spectrum could not be measured with our spectrometer. It was therefore extrapolated with the aid of the pole model. This extrapolated portion amounted to only $(4 \pm 1) \times 10^{-4}$. For the remaining unbound 2^- states in ^{16}N, identified by their counterparts in ^{16}O that are observed in other reactions, we find a combined branching ratio of $(29.9 \pm 1.7) \times 10^{-4}$. Here the state corresponding to the one in ^{16}O at 20.5 MeV dominates with $R_\gamma = (15.1 \pm 1.6) \times 10^{-4}$. [If no continuum background in this region is assumed, an upper limit for the branching ratio for this state of $(21.7 \pm 2.6) \times 10^{-4}$ is obtained and under the same assumption without additional BW resonances a value of $(30.2 \pm 3.7) \times 10^{-4}$]. For the sum of all 1^- states we obtain $R_\gamma = (20.3 \pm 1.4) \times 10^{-4}$, whereby almost half of this value is contributed by the state at $E_x = 22.12$ MeV. When adding the giant-dipole-resonance contributions, i.e., all states with photon energies between 112 and 125 MeV, which correspond to excitation energies for the analog states in ^{16}O between 16 and 28 MeV, one finds $R_\gamma = (45.8 \pm 2.4) \times 10^{-4}$, or $R_\gamma = (76.7 \pm 8.5) \times 10^{-4}$ if the quasi-free contribution is included. For the isovector giant-quadrupole-resonance region, which we take as the energy region between 98 and 113 MeV in our gamma spectrum (corresponding to $E_x = 27$–43 MeV in ^{16}O) (Ref. 4) we obtain $R_\gamma = (64.5 \pm 7.1) \times 10^{-4}$. However, in the absence of structure the excitation of quad-

TABLE II. The experimental partial branching ratios.

E_γ [a]	N_γ [b]	$R_\gamma \times 10^{-4}$ [c]	$R_\gamma \times 10^{-4}$ [d]	Remarks [e]
Resonance contribution				
128	3 642 ± 62	14.5 ± 1.6	15.0 ± 3.0	No separation of 2^-, 0^-, 1^-, 3^-
123.9	583 ± 52	2.3 ± 0.4		Line, $J^\pi = 1^-$
123.2	605 ± 59	2.4 ± 0.4		Line, $J^\pi = 2^-$
121.7	1 110 ± 64	4.4 ± 0.6		Line, $J^\pi = 2^-$
120.5	3 773 ± 92	15.1 ± 1.6	25 ± 6	BW, $\Gamma = 85$ keV, $J^\pi = 2^-$
118.8	2 336 ± 81	9.3 ± 1.2		BW, $\Gamma = 220$ keV, $J^\pi = 1^-$
116.9	1 446 ± 86	5.8 ± 0.8		BW, $\Gamma = 330$ keV, $J^\pi = 1^-$
115.8	731 ± 92	2.9 ± 0.6		BW, $\Gamma = 280$ keV, $J^\pi = 1^-$
114.5	894 ± 91	3.6 ± 0.6		BW, $\Gamma = 350$ keV, $J^\pi = 1^-$, 2^-, (2^+)
Continuum contribution [f]				
125.5	11 731 ± 232	46.8 ± 5.2	184 ± 39	Pole model, $^{15}N(E_x = 0)$, $J^\pi \frac{1}{2}^-$
119.2	30 070 ± 252	120.0 ± 13.0		Pole model, $^{15}N^*(E_x = 6.3$ MeV), $J^\pi = \frac{3}{2}^-$
Total branching ratio				
	56 921 ± 481	227 ± 24	224 ± 48	

[a] Photon energy in MeV.
[b] Number of events in spectrum.
[c] Branching ratio measured in this experiment.
[d] Reference 1.
[e] BW corresponds to Breit-Wigner level shape.
[f] See text.

rupole states is not required. In our parametrization this region is well described by the quasi-free continuum.

Summing over all the contributions yields a total branching ratio of $(2.27\pm 0.24)\times 10^{-2}$, in very good agreement with but more precise than the Berkeley results of $(2.24\pm 0.48)\times 10^{-2}$ and $(2.20\pm 0.33)\times 10^{-2}$ for liquid oxygen and H_2O, respectively, as target.[1]

C. ^{18}O

The photon spectrum from the $^{18}O(\pi^-,\gamma)^{18}N^*$ reaction is shown in detail in Fig. 4. The raw data were processed in the same way as ^{16}O, as far as the cuts on the distributions and subtraction of non-^{18}N-associated background are concerned. However, the resolution here was somewhat higher, with 0.9 at 130 MeV photon energy. Strong transitions that are well separated in the spectrum are observed in the bound state and also in the resonance region. The photon peak with the highest energy corresponds to the ground-state transition in ^{18}N. This state has also been seen in (n,p)- (Ref. 20) and $(t,{}^3\mathrm{He})$- (Ref. 21) charge exchange experiments. The ground state may be either $J^\pi = 0^-$, 1^-, or 2^-. Further excited states in ^{18}N have not yet been observed.[22]

In the isobaric analog nucleus ^{18}O several experimental investigations have been performed in the excitation region of interest between 16 and 26 MeV. Cross sections have been measured for the $^{18}O(\gamma,p)^{17}N$- (Ref. 23) and the $^{18}O(\gamma,n)^{17}O$- (Ref. 24) reactions and also for 180° inelastic electron scattering.[25] The photo reactions show prominent peaks in this region with a fine structure quite similar to the one observed in ^{16}O. The (γ,p) experiments on ^{18}O and ^{16}O manifest a substantial difference between the shapes of the cross sections about 21 MeV. Instead of four narrower and more tightly clustered peaks in ^{16}O, only two broad structures appear in ^{18}O, which may have shoulders or may be composed of two peaks. A similar structure is observed in our experiment.

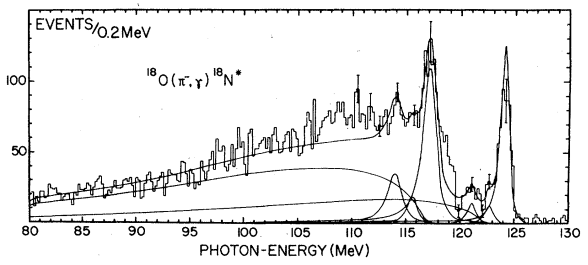

FIG. 4. Photon spectrum of π^- capture in ^{18}O. Solid curve is derived by folding the contributions of the pole models, four Breit-Wigner resonances and two lines with the response function of the apparatus.

The broad bump between 113 and 117 MeV photon energy seen in ^{16}O seems to be distributed over a larger energy region between 105 and 115 MeV in ^{18}O. The upper part of the spectrum, i.e., above 115 MeV, has been analyzed similar to ^{16}O. In Table III the observed transitions are given together with the excitation energies in ^{18}N as well as the analogs in ^{18}O, calculated from the Coulomb energy differences. Furthermore, resonances seen in inelastic electron scattering as well as in (γ,n) and (γ,p) reactions are also listed.

The dominant excitations observed in the bound state and the resonance region at 124.4 and 117.8 MeV photon energy, respectively, correspond to the ground state in ^{18}N and to one strongly excited resonance at an excitation energy of $E_x(^{18}\mathrm{N}) = 6.9$ MeV $[E_x(^{18}\mathrm{O}) = 23.2$ MeV]. Because the (π^-,γ) reaction couples only to protons and the proton shells of ^{16}O and ^{18}O are nearly identical and based on our experiment and theoretical calculations for ^{16}O, according to which 2^- states are excited predominantly, we should assign $J^\pi = 2^-$ to the ground-state excitation in ^{18}N. The same arguments should hold also in the resonance region. Therefore, we assign $J^\pi = 2^-$ to the dominant structure at $E_x(^{18}\mathrm{N}) = 6.9$ MeV. We observe that the separation of this resonance state from the ground state is very close to the energy separation of 6.1 MeV of both dominant $J^\pi = 2^-$ structures in ^{16}O. However, the width of the resonance in ^{18}O is considerably larger than in ^{16}O, suggesting two or more levels. The position coincides with the strongest 1^- excitation seen in the (γ,n) cross section on ^{18}O measurements, while in ^{16}O the strongest 1^- state is observed 2 MeV higher in energy. The disappearance of this separation and the braodening of the resonance at $E_\gamma = 117.6$ MeV may probably be explained by the partial overlap of the 1^- state and the 2^- state in ^{18}O. This is also supported by a comparison of the partial branching ratios.

The branching ratios were deduced by using the method already described. For the quasi-free background, again, we adopt two pole contributions. The recoil nucleus ^{17}N is left either in its ground state $(J^\pi = \frac{1}{2}^-)$ or in its first known excited state with negative parity with $E_x = 5.5$ MeV, $J^\pi = \frac{3}{2}^-$.

The branching ratio for the bound states was found to be $(13.6\pm 1.7)\times 10^{-4}$. It proved impossible to obtain a further separation of bound states with the present statistics and resolution. Comparing the ratio of the partial branching ratio of the bound states to the total branching ratio it appears that the values for ^{18}O and ^{16}O of $(6.7\pm 0.5)\times 10^{-2}$ and $(6.4\pm 0.2)\times 10^{-2}$, respectively, are equal; similarly, we obtain for the total quasi-free contributions

TABLE III. Experimental parameters for radiative pion capture $^{18}O(\pi^-,\gamma)^{18}N$; all energies in MeV. The first column gives the photon energy, the second and the third columns give the excitation energies in ^{18}N and for the analog levels in ^{18}O. The third and the fourth columns list the transitions seen in other experiments, while the last column gives the radiative capture branching ratios.

	$^{18}O(\pi^-,\gamma)^{18}N$		$^{18}O(e,e')^{18}O^*$ [a]	$^{18}O(\gamma,n)^{17}N$ [b]	$R_\gamma \times 10^{-4}$
E_γ	$E_x(^{18}N)$	$E_x(^{18}O)$	$E_x(^{18}O)$	$E_x(^{18}O)$	
124.4	0	16.2	16.6	17.3	12.3 ± 1.6
123.1	1.3 ± 0.2	17.6 ± 0.2	18.4		1.2 ± 0.4
121.5	2.9 ± 0.2	19.2 ± 0.2		19.2	1.4 ± 0.3
			20.2	22.3	
117.5	6.9 ± 0.2	23.2 ± 0.2	21.9	23.4	18.1 ± 2.2
			23.7		
116.0	8.5 ± 0.2	24.8 ± 0.2	25.2	24.2	2.3 ± 0.8
				25.2	
114.3	10.1 ± 0.2	26.4 ± 0.2	26.9	27.5	6.7 ± 0.7
					Pole I 43.6 ± 5.3
					Pole II 110.2 ± 12.6
					Total 196 ± 22

[a] Reference 25.
[b] References 23 and 24.

in ^{18}O and ^{16}O $(77\pm 3)\times 10^{-2}$ and $(74\pm 2)\times 10^{-2}$, respectively. For the strongest resonance excitations at $E_\gamma = 117.6$ MeV (^{18}O) and $E_\gamma = 120.4$ MeV (^{16}O) photon energy we deduce a substantial difference, as the respective values are $(9.2\pm 0.4)\times 10^{-2}$ and $(6.7\pm 0.2)\times 10^{-2}$, taking into account only the strength of the 2^- state in ^{16}O [$E_x(^{16}O) = 20.4$ MeV]. If we add the 1^- strength at the excitation energy of $E_x(^{16}O) = 22.2$ MeV to the 2^- strength, no significant difference in the fractional strength is observed anymore. If we compare the fractional strength in the intervals 106–114 MeV (^{18}O) and 110–118 MeV (^{16}O) we deduce

$$(32\pm 0.5)\times 10^{-2}\ (^{18}O),\quad (36\pm 0.5)\times 10^{-2}\ (^{16}O).$$

Summing over all contributions yields a total branching ratio of $R_\gamma = (1.96\pm 0.22)\times 10^{-2}$, which seems smaller than the one for ^{16}O by 14%.

It is apparent that these slight differences must be due to the two neutrons outside the doubly closed ^{16}O core. One can now speculate that the available transition strength in the GDR region in ^{18}O is distributed over a smaller number of contributing shell-model configurations. To confirm this hypothesis, experiments with improved statistics as well as shell-model calculations would be necessary.

IV. COMPARISON WITH THEORY FOR ^{16}O

1. Transition operator and pionic atom data

For the theoretical analysis of radiative pion capture a standard procedure has now emerged which has recently been reviewed in detail.[26] Taking the transition operator from the elementary process $\pi^- p \to n\gamma$, the impulse approximation is used to calculate transition rates for given nuclear states from the different pionic orbits. For the coefficients of the transition operator, i.e., the relevant linear combination of the pion photoproduction multipoles near threshold, three of the calculations available[4,5,27] use the set of Maguire and Werntz[28]: $A = -0.0332 m_\pi^{-1}$, $B = 0.0048 m_\pi^{-3}$, $C = -0.037 m_\pi^{-3}$, $D = 0.0117 m_\pi^{-3}$, and $E = 0.0304 m_\pi^{-3}$. Ohtsubo *et al.*[3,10] use slightly different values $A = -0.0320\ m_\pi^{-1}$, $B = 0.0075\ m_\pi^{-3}$, $C = -0.0371\ m_\pi^{-3}$, and $D = -0.0140\ m_\pi^{-3}$, whereas Murphy *et al.*[2] limit themselves to the dominant term in the transition operator. The treatment of the pion wave function also differs in the various calculations. In earlier works[2,4,27] hydrogenic wave functions had been used, and the distortion of the pion wave function due to the strong interaction was accounted for only for a multiplicative factor

$$|\phi^{\rm dist}_{\pi,n,l}(0)|^2/|\phi^{\rm hyd}_{\pi,n,l}(0)|^2$$

in the transition rate. Later works[3,5,16] improved this by introducing pion wave functions which are direct solutions of the Klein-Gordon equation for optical potentials. As will be apparent in the following, these differences in the method, however, are not essential and, in particular, do not remove discrepancies with experiment or significantly decrease the sensitivity regarding the specific nuclear wave functions used.

To relate the calculated transition rates to the experimentally observed branching ratios, one has to compute

$$R_\gamma = \sum_{n,l} \frac{\bar{\Lambda}_\gamma^{n,l}}{\Lambda_{\rm tot}^{n,l}} \omega_{n,l} , \tag{1}$$

where $\Lambda_\gamma^{n,l}$ is the calculated radiative transition rate, $\Lambda_{\rm tot}^{n,l}$ is the total absorption rate from a given pionic level including the strong channels, and $\omega_{n,l}$ is the fraction of pions being absorbed from this level. These latter quantities are in principle deduced from the pionic x-ray widths and intensity measurements, supplemented by cascade calculations. As discussed previously,[1,5,26] for light nuclei the sum is limited to two terms $(n,l)=(1,0)$ and $(2,1)$, so that

$$R_\gamma = (1-\omega_{2p})\frac{\Lambda_\gamma^{1s}}{\Lambda_{\rm tot}^{1s}} + \omega_{2p}\frac{\Lambda_\gamma^{2p}}{\Lambda_{\rm tot}^{2p}} . \tag{2}$$

$\Lambda_{\rm tot}^{1s}$ can be determined directly from $\hbar^{-1}\Gamma_{2p-1s}$, for which reliable measurements exist yielding an average value of $(1.16\pm 0.07)\times 10^{19}$ sec^{-1}.[29] ω_{2p} can be approximated by $[1-(Y_{2p}/P_{2p})]$, where Y_{2p} is the yield for the $2p$-$1s$ transition and P_{2p} the population of the $2p$ level. Since Γ_{2p} cannot be measured directly with great precision, it is in general determined from Y_{2p} via

$$\Lambda_{\rm tot}^{2p} = \left(\frac{P_{2p}}{Y_{2p}} - 1\right)\Lambda_{2p-1s}^{\rm em} , \tag{3}$$

where $\Lambda_{2p-1s}^{\rm em} = 6.70\times 10^{14}$ sec^{-1} (Ref. 30) is the calculated electromagnetic transition rate. (The Auger rate is small and neglected here.)

One now obtains

$$R_\gamma = \frac{Y_{2p}}{P_{2p}}\left(\frac{\Lambda_\gamma^{1s}}{\Lambda_{\rm tot}^{1s}} + \frac{\Lambda_\gamma^{2p}}{\Lambda_{2p-1s}^{\rm em}}\right) . \tag{4}$$

For Y_{2p} the available experiments are in considerable disagreement, yielding $Y_{2p}=(4.9\pm 0.7)\times 10^{-2}$ (Ref. 30), $(2.0\pm 0.5)\times 10^{-2}$ (Ref. 31), $(3.0\pm 1.0)\times 10^{-2}$ (Ref. 32), and $(3.4\pm 0.6)\times 10^{-2}$; P_{2p} is found from cascade calculations to be in the range of $(57\pm 6)\times 10^{-2}$ (Ref. 30 and 31).

The corresponding values of Γ_{2p} are then $\Gamma_{2p}=(4.7\pm 0.8)$ eV, (12 ± 4) eV, (8 ± 2) eV, and (7.1 ± 1.3) eV. It is evident that theoretical branching ratios obtained in this manner are subject to a possible error of a factor of 2.5, depending on what value of Y_{2p} one chooses. The only direct measurement of $\Gamma_{2p}=11\pm 6$ eV (Ref. 33) favors the lowest Y_{2p} value which yields $\Gamma_{2p}=12\pm 4$ eV. However, optical model calculations favor $\Gamma_{2p}=(4.7\pm 0.8)$ eV.[34]

The situation is indeed quite unresolved and calls for new experiments. Since the renormalization of the pion wave function at the origin depends mainly on the level shift, not on the width, one does not find the solution for this problem there. When comparing the various theoretical results it seems, therefore, preferable to consider ratios between different contributions rather than absolute branching ratios, since in this case only the small error of $\Lambda_{\rm tot}^{1s}$ enters.

2. *Nuclear wave functions*

(a) Classification of the applied models. The most recent theoretical calculations[5] compare in great detail the various types of nuclear wave functions that have been employed in the past in describing the ^{16}O nuclear structure in general and reactions involving single-body transition operators, in particular, such as μ capture and photoabsorption. The different types of nuclear matrix elements are given by Vergados[4] and Ohtsubo *et al.*[3] We therefore limit our discussion here to a general classification of the wave functions available.

The published papers start with $1\hbar\omega$, 1p-1h excitation for the negative-parity dipole states and the ^{16}O nucleus with the closed-shell component only. Vergados[4] and Ohtsubo *et al.*[3] use single-particle energies and wave functions of Gillet and Vinh Mau[35] in conjunction with the Tamm-Dancoff approximation (TDA). For the residual interaction, Kuo-Lee matrix elements are introduced by Vergados and by Ohtsubo *et al.* In addition, Ohtsubo[3] *et al.* investigate the capture rates also with the random phase approximation (RPA). The single-particle energies adopted by Eramzhyan *et al.*[5] differ slightly from those in the other calculation. All calculations[3-5] (referred to in the following as type I) yield quite similar results. For the positive-parity quadrupole states $2\hbar\omega$, 1p-1h excitations are taken into account by Vergados and Eramzhyan *et al.* In this case the single-particle energies are much more uncertain than for the $1\hbar\omega$ case, where they are fitted to experimental data.

Extensions of this simple model proceed along two lines. First, ground-state correlations (type II models) in the form of 2p-2h admixtures are included in the ^{16}O initial state. Ohtsubo *et al.*[3] follow the approach of Walker,[36] whereas Eramzhyan *et al.*[5] develop their own formalism. These correlations have the effect of reducing the rates

considerably, also in muon capture, where type I calculations notoriously overestimate the capture rate. Finally, admixtures to the 1p-1h excitations are included also for the excited states (type III), namely, 2p-2h ($3\hbar\omega$) admixtures to the dipole states.[3,4] They have the effect of reducing the μ-capture and radiative pion capture rates to the lowest lying dipole states (the bound state quartet) even further and bring the μ-capture rate in agreement with experiment.[5] It should, however, be stressed again that the theoretical calculations mentioned so far do not attempt to calculate the quasi-free capture on an equal level with the resonance transitions. This fact combined with the crude model used by us to subtract the continuum transitions makes a comparison between experiment and theory somewhat tentative. This problem, fortunately, is partly overcome by the recent work of Ohtsuka and Ohtsubo,[19] who apply the continuum shell model.

(b) Bound states. Table IV summarizes the theoretical and experimental branching ratios for the bound-state quartet. It is clear that agreement between our experiment and the theoretical results of Szydlik and Werntz[27] is obtained only for $\Gamma_{2p} = (4.7 \pm 0.8)$ eV. The authors use semiphenomenological, strongly renormalized matrix elements adapted to fit μ capture and inelastic electron scattering data. If the higher Γ_{2p} value is the correct one, then these results fall below the experimental ones, as does the type III calculation. In both cases, however, the experimental rate is overestimated by the simple 1p-1h model, indicating a need for the inclusion of ground-state correlations, as shown previously from μ-capture results.[38] In all theoretical calculations the 1s-capture contribution is small, and the 2^- states dominate with approximately an 80% contribution. In view of the fact that our attempt to separate the closely bunched states yielded about equal contributions for the 2^- and 3^- states, an experiment with even higher resolution would appear desirable in order to resolve this discrepancy. It should be remarked here that other charge-exchange reactions such as (t, ^{3}He) (Ref. 39) yield $I(3^-)/I(2^-) \simeq 2:1$ at momentum transfers of about 190 MeV/c and electron scattering[40] indicates a strong dependence of the 3^--form factor upon the momentum transfer.

(c) Dipole transitions. Table V shows the theoretical and experimental branching ratios for the sum of all $J^\pi = 1^-$ and for the sum of all $J^\pi = 2^-$ transitions in the giant-resonance region. In addition, the branching ratio divided by the bound-state-quartet branching ratio is given. The following conclusion can be drawn: Using $\Gamma_{2p} = (4.7 \pm 0.8)$ eV, the branching ratios for the sum of all 2^- states exceed the experimental one by factors of 2.5 to 4, and up to 2 for the 1^- states. These differences lie outside the uncertainties introduced by the treatment of the continuum. The high Γ_{2p} value of (12 ± 4) eV yields good agreement for the 2^-

TABLE IV. Theoretical branching ratios for the bound-state quartet in ^{16}N. The second and the third columns give the theoretical radiative transition rates, which are then converted to branching ratios using Eq. (4). These are given in the fourth and the fifth columns for the two capture schedules available.

Type [a]	Λ_γ^{1s} (10^{16} sec^{-1})	Λ_γ^{2p} (10^{12} sec^{-1})	R_γ [b] (10^{-4})	R_γ [c] (10^{-4})	f_{1s} [d] (%)	f_{2^-} [e] (%)	Reference
			14.5 ± 1.6				Experiment
I	6.02	32.89	20 ± 7	47 ± 8	9.4	83	Ref. 5, case A
I	6.45	33.78	21 ± 8	48 ± 8	9.8	85	Ref. 3, TDA
I	9.66	19.64	18 ± 6	40 ± 7	8.7	88	Ref. 4 [f]
I	5.84	30.84	19 ± 6	44 ± 8	9.8	83	Ref. 3, RPA
II	4.02	21.31	13 ± 4	33 ± 6	9.1	81	Ref. 5, case B
II	3.63	18.32	12 ± 4	26 ± 5	10.2	72	Ref. 3, using Walker
III	2.80	15.13	10 ± 3	23 ± 4	8.7	79	Ref. 5, case C
	1.76	10.36	6 ± 2	15 ± 3	8.8	86	Ref. 27 [g]

[a] Indicates a general classification of nuclear wave functions (see text).

[b] Using $\Gamma_{1s} = (7.56 \pm 0.5)$ keV, $\Gamma_{2p} = (12 \pm 4)$ eV, Ref. 31.

[c] Using $\Gamma_{1s} = (7.56 \pm 0.5)$ keV, $\Gamma_{2p} = (4.7 \pm 0.8)$ eV, Ref. 30.

[d] Contribution of 1s capture to total branching ratio with $\Gamma_{1s} = (7.56 \pm 0.5)$ keV, $\Gamma_{2p} = (4.7 \pm 0.8)$ eV.

[e] Contribution of $2^- - ^{16}$N-ground state to total branching ratio with $\Gamma_{1s} = (7.56 \pm 0.5)$ keV, $\Gamma_{2p} = (4.7 \pm 0.8)$ eV.

[f] Correction factors $C(1s) = 0.45$ and $C(2p) = 1.45$, included.

[g] Using semiphenomenological matrix elements.

TABLE V. Theoretical branching ratios for dipole transitions. (For an explanation of symbols see Table IV.)

Type[a]	$\Lambda_\gamma^{1s}(1^-)$ (10^{16} sec^{-1})	$\Lambda_\gamma^{2p}(1^-)$ (10^{12} sec^{-1})	$R_\gamma(1^-)$[b] (10^{-4})	$R_\gamma(1^-)$[c] (10^{-4})	$\Lambda_\gamma^{1s}(2^-)$ (10^{16} sec^{-1})	$\Lambda_\gamma^{2p}(2^-)$ (10^{12} sec^{-1})	$R_\gamma(2^-)$ (10^{-4})	$R_\gamma(2^-)$[b] (10^{-4})	$R_\gamma(1^-)/R_\gamma$(b.s.)[d]	$R_\gamma(2^-)/R_\gamma$(b.s.)[d]	References
				20.3 ± 1.4				21.9 ± 1.7	1.40 ± 0.05	1.51 ± 0.04	Experiment
				23.9 ± 1.5				25.5 ± 1.8	1.64 ± 0.05	1.75 ± 0.05	Experiment[e]
I	12.24	25.72	20 ± 7	42 ± 7	12.15	65.60	42 ± 14	93 ± 16	0.90	1.99	5, case A
I	14.49	27.60	22 ± 8	43 ± 7	13.20	69.70	26 ± 9	98 ± 16	0.90	2.04	3, TDA
I	31.98	18.28	22 ± 8	43 ± 7	23.36	50.18	41 ± 13	101 ± 16	1.08	2.52	4, f
I	13.13	24.76	21 ± 8	42 ± 7	11.76	62.10	38 ± 13	89 ± 15	0.95	2.02	3, RPA
II	7.85	16.23	12 ± 4	27 ± 5	7.54	41.18	26 ± 9	59 ± 11	0.56	1.23	5, case B
II	13.63	26.37	19 ± 5	44 ± 7	12.96	67.50	40 ± 10	96 ± 16	1.69	3.69	3, 36
III	8.24	14.84	12 ± 4	25 ± 6	8.11	44.06	27 ± 6	63 ± 12	1.09	2.74	5, case C

[a] Indicates general classification of nuclear wave functions (see text).
[b] Using $\Gamma_{1s} = (7.56 \pm 0.5)$ keV, Ref. 29, $\Gamma_{2p} = (12 \pm 4)$ eV, Ref. 32.
[c] Using $\Gamma_{1s} = (7.56 \pm 0.5)$ keV, $\Gamma_{2p} = (4.7 \pm 0.8)$ eV, Ref. 31.
[d] Branching ratio divided by branching ratio of bound-state quartet, this number is independent of the capture schedule.
[e] Modified ratio, when the contribution of an unidentified state is included [$E^*(^{16}\mathrm{N}) = 13.24$ MeV].
[f] Correction factors included $C(1s) = 0.45$, $C(2p) = 1.45$.

states between theory and experiment, particularly for type II and type III models only; however, the 1^- branching ratios are underestimated in this case. From the relative branching ratios to the bound-state quartet, it again seems that the 1^- strength is underestimated. Closest to observation in this case are type II models, whereas in the type III models the bound-state transitions are relatively too strongly suppressed. This might indicate that at least the 2^- states are of rather pure 1p-1h configuration. This statement is further supported, if one considers the distributions of the 1^- and 2^- strength over the different states are displayed in Fig. 5 and Fig. 6. For the 2^- states a straightforward and relatively unambiguous picture emerges. The theoretical states expected by Eramzhyan *et al.* at 18.0, 18.2, and 19.6 MeV and by Ohtsubo *et al.* at 17.7, 19.3, and 20.4 MeV find their experimental counterparts at 17.7, 19.0, and 20.4 MeV with approximately the right distribution of strength. The 20.4-MeV state, consistently predicted in all types of models with the dominant strength, is rather nicely confirmed experimentally. The configuration of this state is mainly $0.75|D_{5/2}P_{3/2}^{-1}\rangle + 0.60|S_{1/2}P_{3/2}^{-1}\rangle$. Even in the very early simple Goldhaber-Teller model calculation[2] this resonance is predicted. It was already seen in the old radiative π-capture measurements; even the low-statistics $(\pi^-, \gamma n)$-coincidence experiment[43] shows clear evidence in the neutron spectrum for the decay of this state. Around 23 to 24 MeV a further 2^- state is expected, which could be tentatively identified with the state at 24.1 MeV,

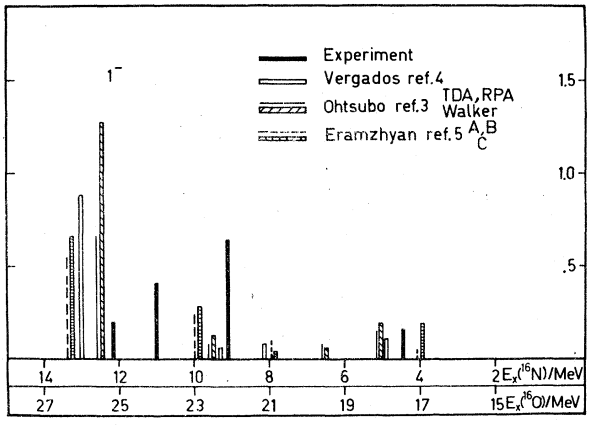

FIG. 5. Comparison of the experimental ratio $R\gamma\,(1^-)/R\gamma$ (b.s.) to the theoretical results of Vergados (Ref. 3), Ohtsubo (Ref. 4), and Eramzhyan (Ref. 5). The results of the TDA and RPA calculations of Ohtsubo are not significantly different, so that only the TDA results are shown. Also, in Eramzhyan's calculations for model A and B no difference is found. Again only the result of model B is shown.

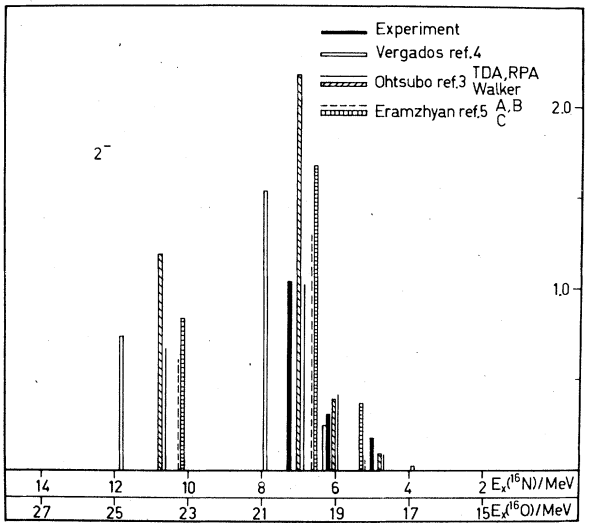

FIG. 6. Comparison of the experimental ratio $R\gamma(2^-)/R\gamma$ (b.s.) to the experimental results of Refs. 3, 4, and 5.

found in the experiment for which no spin assignment could be performed by comparison of experimental results.

Regarding the 1^- states, according to the theory most of the strength is concentrated near 26 MeV (relative to ^{16}O), with smaller contributions at 17.5, 20.5, and 23 MeV. Our experiment shows states near 17, 22, 24, and 25 MeV, whereby only the transition to the lowest level has a strength that is in agreement with theory.

The energy of the most strongly excited state seen in our experiment corresponds precisely to the energy of the strongest peak in the photonuclear giant resonance in ^{16}O at 22.2 MeV. As already mentioned, the giant dipole resonance which is excited in photonuclear reactions and related processes is an isospin mode. Such a mode, according to the available calculations, should differ in energy from the spin-isospin mode excited in pion capture by several MeV. Vergados,[4] e.g., quotes for the principal component of the isospin resonance an energy of 23.9 MeV and for the spin-isospin case 26.5 MeV. However, such calculations should not be taken too literally, because they presuppose almost pure 1p-1h configurations. On the other hand, from the extensive work on photonuclear reactions on ^{16}O it is well known that 3p-3h configurations must be included to account for the several peaks in the giant resonance,[41] and at least 2p-2h configurations are necessary for explaining the partial decay of this giant resonance to even-parity states in ^{15}N and ^{15}O.[42] Vergados pointed out that the distinction between spin-flip and non-spin-flip states in non-closed-shell nuclei is no longer meaningful due to recoupling and antisymmetric effects. Our data therefore seem to support the assumption that the 1^- states in ^{16}O have a considerably more complicated structure than considered in the past in calculations for radiative pion capture. Thus, we do not believe that this initially puzzling coincidence in energy found in the different experiments is fortuitous.

(d) Quadrupole transitions. The transitions to positive parity states ($2\hbar\omega$) are not as easily identifiable, since they are expected to be broad and, furthermore, they are spread over a large energy region. It is apparent from our parametrization of the spectrum that there is no compelling need for invoking their presence; the spectrum shape follows the pole model nicely. In the work of Eramzhyan *et al.*,[5] which includes a complete diagonalization of the $2\hbar\omega$ subspace, 462 such states are expected below 115-MeV photon energy. With this high number of states an attempt to distinguish them from the continuum becomes pointless. Table VI gives a comparison of the theoretical branching ratios with the total experimental rate for the region below 115 MeV photon energy. From the relative branching ratios, assuming the most reasonable model for the bound-state transitions, one may deduce that only 60% of the observed rate can be accounted for by quadrupole transitions.

(e) Continuum shell-model calculations. Othsuka and Ohtsubo[19] made an attempt to overcome the problem of the background treatment. They adopted the continuum shell model of Birkholz *et al.*[37] and treated thus the resonances and the quasi-free emission of a nucleon consistently. They assumed that the ground state of ^{16}O is described by the Walker model and the configuration space is limited to 1p-1h excitation only. The single-particle potential and the residual interaction are taken from Raynal *et al.*[44]

Othsuka's and Ohtsubo's result is plotted together with the experimental data in Fig. 7. The smooth lines show the total spectrum as well as the contribution of the negative parity states (0^-, $1^-, 2^-, 3^-$) and the contribution of the continuum, all folded with the response function of our apparatus. The total theoretical strength $R_\gamma = 3.04\times10^{-2}$ was normalized to the experimental value $R_\gamma = (2.27\pm0.24)\times10^{-2}$. It is evident that the excited resonances are well reproduced. Even the predicted widths of the resonances are in agreement. The 19% of the total radiative capture rate due to the 1^- strength seems underestimated. Too much strength is concentrated in the 2^- excitation (~48%), especially in the resonance at 120 MeV photon energy. The contributions of the 0^- excita-

TABLE VI. Theoretical branching ratios for quadrupole transitions (positive parity states). (For an explanation of symbols see Table IV.)

Λ_γ^{1s} (10^{16} sec^{-1})	Λ_γ^{2p} (10^{12} sec^{-1})	R_γ [a] (10^{-4})	R_γ [b] (10^{-4})	f_{1s} [c] (%)	f_{1^+} [d] (%)	f_{2^+} [d] (%)	R/R(b.s.) [i]			References
6.5	94.5	51±13	125±22	3.8	18	37	5.84 [e]	4.13 [f]	2.68 [g]	5, case D
4.5	68.2	37± 9	91±16	3.7	18	37	4.21	3.00	1.94	5, case E
7.8	51.2	40±10	98±16	2.4	12	41		2.21		4
13.7	65.7	38±10	93±16	10.7	11	37				2
			64.5±7.1					4.4±0.7		Experiment [h]

[a] Using $\Gamma_{1s}=(7.56\pm0.5)$ keV, $\Gamma_{2p}=(12\pm4)$ eV, Ref. 32.
[b] Using $\Gamma_{1s}=(7.56\pm0.5)$ keV, $\Gamma_{2p}=(4.7\pm0.8)$ eV, Ref. 31.
[c] Contribution of $1s$ capture to total branching ratio [$\Gamma_{2p}=(4.7\pm0.8)$ eV].
[d] Contribution of 1^+ (2^+) states to total branching ratio.
[e] Bound-state branching ratio case C.
[f] Bound-state branching ratio case B.
[g] Bound-state branching ratio case A.
[h] Contribution in energy region 98 MeV$\leq E\leq$113 MeV.
[i] Relative to bound state.

tion (0.2%) and the 3^- excitation (2%) are negligible. Roughly 70% of the available strength is concentrated in resonance excitation.

The separate study of the quasi-free transitions for different values of total angular momentum $\vec{J}=(\vec{j}_n+\vec{j}_N)_J$ resulting from the coupling of neutron wave $j_n=l_n\pm\frac{1}{2}$ and the residual nucleon states J_N is based on parity and excitation energy. Ohtsubo et al.[18] find that the strong transitions are to channels with $J_N^\pi=\frac{1}{2}^-$, $J_N^\pi=\frac{3}{2}^-$, and $l_N=1$ and 3. Those channels are labeled by (J,l_n). This effect is clearly observed in the $(J,l_n)=(3,f)$ and $(J,l_n)=(1,p)$ channels.

In the last case interference is observable. Furthermore, at lower photon energies (<100 MeV) these curves show no significant deviation from the pole-model treatment. This model therefore provides a nice *a posteriori* justification for the simple approximation used to extract the experimental branching ratios. It is clear, however, that one overestimates the quasi-free contribution by using the pole model only. The continuum shell-model calculation gives rise to quasi-free transitions only for 30% of all captures. The main contributions are to the $(J,l_n)=(3,f)$ state with 12% and to the $(J,l_n)=(1,p)$ and $(J,l_n)=(2,f)$ state with approximately 8% each, whereas the $(J,l_n)=(2,p)$ contribution of 2% is negligible. In general, the sum of these four contributions reproduces nicely the spectrum shape between 80 and 110 MeV. If one uses a different method of normalization, for example, adjusting the strength between 113 and 125 MeV, the measured spectrum in the GDR region is reproduced reasonably well, but the 1^--excitation strength is underestimated and the strength between 98 and 113 MeV is also too low. This may be caused by the fact that the giant-quadrupole-resonance excitation is not included in that particular model.

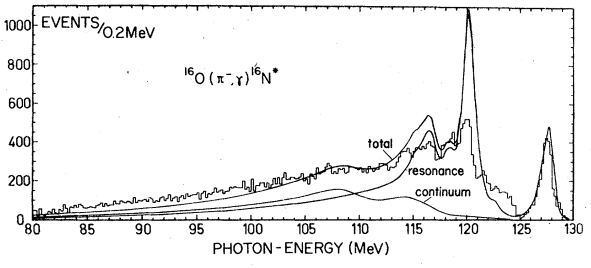

FIG. 7. Comparison of the photon spectrum for ^{16}O with the results of the continuum shell-model calculation (Ref. 10).

V. CONCLUSIONS

The data presented here demonstrate anew that the radiative pion capture reaction may serve as a favorable tool in studying isovector transitions in light nuclei. While previous data[26] have emphasized mainly the selectivity of this reaction in exciting analogs of $M1$-type transitions in p-shell nuclei, $M2$ and to a lesser extent $E1$ transitions are shown to be the dominant structures for ^{16}O and ^{18}O here. The sensitivity to a particular type of transition with large spin-density matrix elements compensates the restriction to a fixed momentum transfer in the (π^-,γ) data, sometimes consided a severe limitation, if this process is compared to more traditional electromagnetic processes such as inelastic electron scattering. Of course the muon capture process, whose axial

part resembles closely the dominant part of the radiative pion capture transition operator, is theoretically expected to show similar selectivity,[45,46] but it is experimentally not accessible to the type of high-resolution spectroscopy which are new detector allows. The comparison of our data with available shell-model calculations shows that the general structure of the data can be explained well, but a detailed fit and thus a useful set of phenomenological wave functions can only be obtained when all electromagnetic and weak processes involving the same transitions are considered concurrently. An annoying problem in the comparison between theory and experiment persists in the fact that $2p$-capture calculations are more model dependent and that pionic capture schedules needed to relate them to the experimental data are badly known. This can be circumvented in future experiments, isolating $1s$ capture via a coincidence with the x-rays feeding the $1s$ level. This technique has successfully been applied by us to ^{6}Li.[47] Future work should also consider coincidence angular correlation experiments with the decay neutrons from the unbound states as well as secondary nuclear γ rays as recently proposed.[48] Then it should be possible to extract spin and parity assignments directly from (π^-, γ) data, and thus fully exploit the capability of this reaction.

ACKNOWLEDGMENTS

The authors wish to express their gratitude to Professor C. Zupancic of the University of Munich for his constant support of this experiment and to Mr. A. Frischknecht and Mr. W. Stehling, who helped during the data taking. We benefited from discussions about theoretical aspects with Dr. J. Meier-ter Vehn. The authors are extremely grateful to Dr. R. A. Eramzhyan, Dr. M. Gmitro, and to Professor H. Ohtsubo and Professor J. D. Vergados, who not only sent us the results of their calculations before publication but also found the time to patiently explain them to us. We gratefully acknowledge the support of the SIN laboratory under the directorate of Professor J. P. Blaser. One of the authors (H. A. Medicus) visiting at SIN wishes to acknowledge the hospitality extended to him during this stay. This work was supported in part by the Swiss National Foundation and the German Bundesministerium für Forschung und Technologie.

---

*Present address: Laboratory for High Energy Physics, Swiss Federal Institute of Technology, Zürich, c/o SIN, CH-5234 Villigen, Switzerland.
†Present address: Physik-Institut der Universität, Zurich, CH-8001 Zürich, Switzerland.

[1]J. A. Bistirlich *et al.*, Phys. Rev. C 5, 1867 (1972).
[2]J. D. Murphy *et al.*, Phys. Rev. Lett. 19, 714 (1967).
[3]H. Ohtsubo, T. Nishiyama, and M. Kawaguchi, Nucl. Phys. A224, 164 (1974).
[4]J. D. Vergados, Phys. Rev. C 12, 1278 (1975).
[5]R. A. Eramzhyan, M. Gmitro, R. Sakaev, and L. A. Tosunjan, Nucl. Phys. A290, 294 (1977).
[7]J. C. Alder *et al.*, Nucl. Instrum. Methods 160, 93 (1979).
[7]J. C. Alder *et al.*, Helv. Phys. Acta 51, 91 (1978).
[8]H. Davies, H. Muirhead, and J. N. Woulds, Nucl. Phys. 78, 673 (1966).
[9]L. G. Dakhno and Yu. D. Prokoshkin, Yad. Fiz. 7, 565 (1968) [Sov. J. Nucl. Phys. 7, 351 (1968)].
[10]U. Kneisel *et al.*, Nucl. Instrum. Methods 127, 1 (1975).
[11]W. J. O'Connel, G. L. Latshaw, J. J. Black, and S. S. Hanna, in *Proceedings of the International Conference on Photonuclear Reactions and Applications, Asilomar, 1973*, edited by B. L. Berman (Lawrence Livermore Laboratory, Univ. of California, 1973), Vol. II, p. 939.
[12]A. Veyssière *et al.*, Nucl. Phys. A227, 513 (1974).
[13]R. L. Bramblett, J. T. Caldwell, R. R. Harvey, and S. C. Fultz, Phys. Rev. 133, B869 (1964).
[14]J. T. Caldwell, R. R. Harvey, R. L. Bramblett, and S. C. Fultz, Phys. Lett. 6, 213 (1963).
[15]V. P. Denisov, A. P. Komar, and L. A. Kulchitsky, Nucl. Phys. A113, 289 (1968).
[16]M. Stroetzel and A. Goldman, Z. Phys. 233, 245 (1970).
[17]A. R. Barnett and N. W. Tanner, Nucl. Phys. A152, 257 (1970).
[18]S. H. Chew, J. Lowe, J. M. Nelson, and A. R. Barnett, Nucl. Phys. A229, 241 (1974).
[19]N. Ohtsuka and H. Ohtsubo, in *Proceedings of the International Conference on Nuclear Structure, Tokyo, 1977*, edited by T. Marumori (Physical Society of Japan, Tokyo, 1978), and private communication; Nucl. Phys. A306, 513 (1978).
[20]L. F. Chase, Jr., H. A. Greuch, R. E. McDonald, and F. J. Vaugun, Phys. Rev. Lett. 13, 665 (1964).
[21]R. H. Stokes and P. G. Young, Phys. Rev. 178, 1789 (1969).
[22]F. Ajzenberg-Selove, Nucl. Phys. A190, 1 (1972).
[23]B. L. Berman, D. D. Faul, R. A. Alvarez, and P. Meyer, Phys. Rev. Lett. 36, 1441 (1976) and private communication.
[24]U. Kneissel, K. H. Leister, H. O. Neidel and A. Weller, Nucl. Phys. A272, 125 (1976).
[25]G. J. Vanpraet, Phys. Lett. 17, 120 (1965).
[26]H. W. Baer, K. M. Crowe, and P. Truöl, Adv. Nucl. Phys. 9, 177 (1977).
[27]P. Szydlik and C. Werntz, Phys. Lett. 51B, 209 (1974).
[28]W. Maguire and C. Werntz, Nucl. Phys. A205, 211

(1973).
[29]G. Backenstoss, Annu. Rev. Nucl. Sci. 20, 467 (1970).
[30]H. Koch *et al.*, Phys. Lett. 28B, 279 (1968).
[31]W. W. Sapp, Jr., M. Eckhause, G. H. Miller, and R. E. Welsh, Phys. Rev. C 5, 690 (1972).
[32]M. Camac, A. D. McGuire, J. B. Platt, and H. J. Schulte, Phys. Rev. 99, 897 (1955).
[33]T. von Egidy and H. P. Povel, Nucl. Phys. A232, 511 (1974).
[34]M. Krell and T. E. O. Ericson, Nucl. Phys. B11, 521 (1969).
[35]V. Gillet and N. Vinh Mau, Nucl. Phys. 54, 321 (1964).
[36]G. E. Walker, Phys. Rev. 174, 1290 (1968); Phys. Rev. C 5, 1540 (1972).
[37]J. Birkholz, Nucl. Phys. A189, 385 (1972).
[38]For a review see N. Mukhopadhyay, Phys. Rep. 30C, 1 (1977).
[39]E. R. Flynn and J. D. Garret, Phys. Rev. C 10, 409 (1974).
[40]J. C. Kim, R. P. Singnal, and H. S. Kaplan, Can. J. Phys. 48, 83 (1970).
[41]C. M. Shakin and W. L. Wang, Phys. Rev. Lett. 26, 902 (1971).
[42]R. O. Owens and J. E. R. Baglin, Phys. Rev. Lett. 17, 1268 (1966).
[43]J. C. Alder *et al.*, Lett. Nuovo Cimento 4, 256 (1970).
[44]J. Raynal, M. A. Melkanoff, and T. Sawada, Nucl. Phys. A101, 396 (1967).
[45]M. Gmitro, R. A. Sakaev, L. A. Tosunjan, R. A. Eramzhyan, Dubna Report No. P2-11511, 1978 (unpublished).
[46]N. Mukhopadhyay, Phys. Rep. 30C, 1 (1977).
[47]D. Renker *et al.*, Phys. Rev. Lett. 41, 1279 (1978).
[48]M. Gmitro, L. A. Tosunjan, and R. A. Eramzhyan, Dubna Reports Nos. P2-11549, 1978 (unpublished), P2-11562, 1978 (unpublished) and P2-11511, 1978 (unpublished).